

## **HF-BAND WIRELESS POWER TRANSFER SYSTEM: CONCEPT, ISSUES, AND DESIGN**

**B.-J. Jang<sup>1</sup>, S. Lee<sup>2</sup>, and H. Yoon<sup>3,\*</sup>**

<sup>1</sup>Dept. of Electrical Eng., Kookmin University, 861-1, Jeongneung-dong, Seongbuk-gu, Seoul 136-702, Korea

<sup>2</sup>Dept. of Information and Communication Eng., Sejong University 98 Gunja-dong, Gwangjin-gu, Seoul 143-747, Korea

<sup>3</sup>Dept. of Computer and Electronic Eng., Myongji College, 356-1 HONGEUN2-dong Seodaemun-gu, Seoul 120-776, Korea

**Abstract**—High-frequency (HF) band wireless power transfer systems offer the promise of cutting the last cord, allowing users to seamlessly recharge mobile devices as easily as wireless communication. Yet there are still many technical issues that need to be overcome. Among them, one of the most difficult problems is maintaining impedance match over a short range, where the distance between a transmitter and receiver could vary. In this paper, the effect of impedance mismatch of a HF-band wireless power transfer system is carefully investigated and two compensation methods are suggested to overcome this within a short range, where frequent impedance mismatch can occur. Each method has pros and cons. In order to verify the feasibility of the proposed methods, HF-band wireless power transfer systems, with a pair of rectangular loop resonators, were designed. The efficiency and input impedance variation were simulated and measured. From these results, proposed methods show enhanced efficiency performance than a typical wireless power transfer system without any compensation circuits.

### **1. INTRODUCTION**

In recent years, wireless power transfer (WPT) systems that operate in a high-frequency (HF) band have drawn a great deal of attention. Especially, the use of mobile devices, such as cellular phones, tablet computers, etc., have justified the necessity of WPT. Because the

---

*Received 5 December 2011, Accepted 11 January 2012, Scheduled 19 January 2012*

\* Corresponding author: Hyungoo Yoon (hgyoon@mjc.ac.kr).

existing electrical-wire grid carries power almost everywhere, a WPT device operating in a short range less than 1 m could be quite useful for these mobile devices [1].

Generally, it is well known that there are three types of WPT: radio frequency (RF) radiation, inductive coupling in low frequency (LF) bands, and a resonant coupling in HF-bands [2]. RF radiation, although suitable for exchanging information, can transfer only small amounts of power (several mill-watts), because a majority of power is lost to free space. RF radiation using high directional antennas could be used for WPT, even over long distances, but requires the existence of an uninterrupted line-of-sight that may harm the human body [3]. On the other hand, LF-band inductive coupling can transfer power with high efficiency but over a very short range (several centimeters) [4]. Recently, an industry consortium has been formed to standardize this technology for charging mobile devices [5].

The last type of WPT, HF-band resonant coupling, can transfer high power over a short range (within 1 or 2 meters). For example, Marin Soljacic of MIT and his team have demonstrated how a 60-Watt light bulb could be wirelessly powered from a distance of 2 m using the resonant frequency of 10 MHz [6]. The reported efficiency was about 40% at a distance of 2 m. Mid-2008, researchers at Intel presented a similar experiment, reporting an increased efficiency of 75% at a similar power level, but at a shorter distance of 1 m [7]. By using negative permeability metamaterial structures, the efficiency of energy transmission was approximately 80% at a transmission distance of 1.5 m [8]. The basic principle of this technology is that two separate resonators with the same resonant frequency can exchange power efficiently, while the coupling effect is weak between objects with different resonant frequencies. Whereas the reported maximum separation distance for resonant coupling is within 1 or 2 meters, they created expectations for a system that could provide power in a larger space similar to wireless communication networks, such as Wireless LAN, Bluetooth, etc.. Because an electrical-wire grid exists almost everywhere in homes and offices, even a WPT device operating in a range less than 1 m could be quite useful for charging mobile devices. Characteristics of the three WPT systems are summarized in Table 1.

But, in general, a HF-band resonant WPT system shows impedance variations within a short range, because the coupling coefficient changes with respect to the separation distance between two resonators. As the separation distance between two resonators decreases, the greater the coupling coefficient. Then, the effect of impedance mismatch increases because the reflected impedance changes depending on the degree of coupling. Therefore, the power

**Table 1.** Comparison of different wireless power technologies.

	Induction Coupling	Resonant Coupling	Radiative Transfer
Wave	Magnetic field (Wideband)	Magnetic field (Narrow band)	Electro-magnetic wave
Range	Very short ( $\sim$ cm)	Short ( $\sim$ m)	Medium and Long ( $\sim$ km)
Efficiency	High	Medium	Low
Operating Frequency	LF-band ( $\sim$ several hundred kHz)	HF-band (6.78 MHz, 13.56 MHz)	RF-band (2.4 GHz, 5.8 GHz)
Typical Load	Varying load (battery)	Fixed Impedance	Fixed Impedance
Advantage	High Efficiency	Medium efficiency in a short range	Long range
Bottleneck	Very short range	Difficulties in maintaining high $Q$	Low efficiency, Human Safety

transfer efficiency of a HF-band WPT system can be improved by reducing this impedance mismatch. On the other hand, due to the impedance mismatch, there exist two resonance frequencies (even and odd modes) that permit maximum power efficiency over a short range. Therefore, the power transfer efficiency of the WPT system can also be improved by varying the operating frequency of the WPT system adaptively according to the separation distance. In particular, the efficiency can be dramatically enhanced over a very short range where large impedance mismatch occurs [9, 10].

In this paper, the concept and issues related to HF-band WPT systems are explained using a simplified equivalent circuit model. Impedance mismatching effects are focused on in great detail. Two efficiency enhancements for a HF-band WPT system to reduce impedance mismatch are proposed. One method is to vary the output frequency of a voltage-controlled oscillator (VCO), depending on the separation distance, to create an adaptive-frequency control circuit [11]. The other method is to use a tunable impedance matching circuit using varactor diodes according to the separation distance between two resonators [12]. All these methods can compensate for the impedance-mismatching effect in the short range, where large impedance mismatch occurs. In order to verify the feasibility of the proposed methods, HF-band resonant WPT systems with rectangular loop resonators were designed and their impedance characteristics

carefully investigated from the measured results. This paper is organized as follows: In Section 2, the general structure of a WPT system is reviewed, and the characteristics of HF-band resonant WPT systems are carefully investigated and compared with their LF-band counterparts. Section 3 explains various technical issues in a HF-band WPT system using an equivalent circuit model. Two efficiency enhancement methods of a HF-band WPT system to compensate for the impedance mismatch are proposed in Section 4. Experimental results are also included. Finally, Section 5 presents the conclusion of this paper.

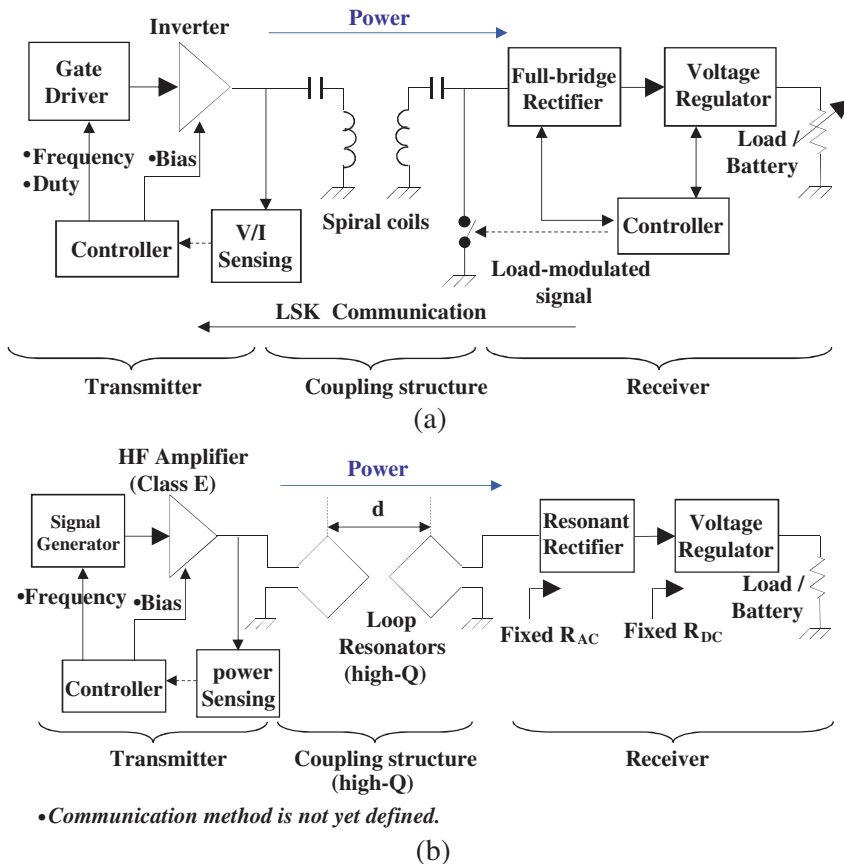


**Figure 1.** Configuration of the WPT system consisting of a transmitter (left), the coupling structure (middle), and the receiver (right). (a) Induction coupling in LF-band WPT system with two high- $Q$  coils and a varying load. (b) Resonant HF-band WPT system with two high- $Q$  loop resonators with a fixed load.

## 2. CONCEPT OF HF-BAND WPT

### 2.1. Comparison of LF- and HF-WPT

Figures 1(a) and 1(b) show the configurations of LF- and HF-band WPT systems, respectively. Generally, the WPT system consists of a transmitter and a receiver, and a coupling structure. Power transfer always takes place from the transmitter to the receiver.

The LF-band WPT system consists of a full- or half-bridge inverter for the transmitter, coupling coils, and a full-bridge rectifier and a regulator for the receiver. Although the LF-band system may contain multiple transmitters or receivers, a transmitter can serve only a single receiver at a given time. The coupling structure consists of multi-turn spiral coils with high quality factor ( $Q$ ) values, which consist of a primary coil in the transmitter and a secondary coil in the receiver. In fact, the primary coil and secondary coil form two halves of a coreless resonant transformer. To create resonance, a lumped capacitor is normally added. Appropriate shielding on the bottom face of the primary coil and the top face of the secondary coil, as well as the close spacing of the two coils, ensures that power transfer occurs with a high efficiency.

LF-band WPT systems have two primary functional units, namely a power conversion unit and a communication and control unit. Because a LF-band WPT system is generally designed to charge a battery, load resistance can vary according to its charging level. Therefore, various control mechanisms are commonly used to adjust the transferred power to the requested level in the battery. Also, as a result of varying load resistance, the overall  $Q$  of a LF-band WPT system lowers, even though the  $Q$  values of the coils are high. Generally, the control mechanisms are classified in three different ways: a frequency control, a duty cycle control, and a voltage control. For example, the frequency control adjusts the switching frequency of the gate driver to control the amount of transferred power, which is dependent on the switching frequency due to the resonant nature of the coils. Contrary to the direction of the power transfer, the communication direction is from receiver to transmitter [5].

On the other hand, the HF-band WPT system consists of a HF-band amplifier, loop resonators, and resonant rectifier circuit. When the power of the HF-band amplifier is on, the resonant alternating current (AC) excites the transmitter's loop resonator, which stores power in the same manner as a discrete LC resonator tank. A magnetic field interaction occurs between the two resonators. As the loop resonators are magnetically coupled, a mutual inductance is induced which is a function of the shape of the resonators and separation

distance ( $d$ ) between them. Finally the received power is transferred to a fixed load via a resonant rectifier. In the HF-band, the transmitter coupling structure consists of a single — or small number of turns — loop resonator with an impedance matching network. As the operating frequency is higher than the LF-band counterpart, the loop resonator can be designed with very high  $Q$  values. Also, load resistance in HF-band WPT systems may be fixed in order to maintain high  $Q$  values in the overall system. Until now, the communication and control methods in HF-band WPT systems have not been standardized yet.

## 2.2. Design Examples of LF- and HF-WPT

As shown in Table 1 and Fig. 1, a main difference between LF- and HF-band WPT is overall  $Q$  value. Although the  $Q$  values of coils or resonators of two systems are the same, the overall  $Q$  of a LF-band WPT system is lower than that of a HF-band counterpart at the cost of having the ability to control varying load profiles. In contrast, the load resistance should be fixed for a HF-band WPT system at the expense of no load control mechanism. Owing to this high- $Q$  value, HF-band WPT systems have a relatively long range compared to LF-band systems. By analogy, it is possible to imagine that if the load resistance is fixed, an LF-band WPT system may have a relatively long distance, too.

On the other hand, as the operation frequency of a HF-band WPT system is tens times higher than that of a LF-band; the resonator could be made by loops with a small number of turns. Therefore, the  $Q$  value of a HF-band resonator is relatively higher than that of a LF-band coil. As a result of relatively long wires and eddy current loss between the trace of coils, the resistance of a LF-band coil is relatively higher than a HF-band resonator. Therefore, they have relatively low  $Q$  values [13]. Similarly, if a large coil can be made to reduce eddy current crowding effect in a LF-band, the coil of the LF-band has relatively high  $Q$  values.

Figure 2 shows the photographs of typical LF- and HF-band WPT systems. In the LF-band system, which is manufactured by Texas Instruments<sup>TM</sup> the maximum output power is 5 W having 70% full-load efficiency. The receiver coil should be properly located on the top of the transmitter coil in order to maintain the high efficiency. If not, the efficiency can be dramatically decreased. The output diameter of the transmitter coil is just around 40 mm. The coil is a wire-wound type, and consists of no. 20 AWG (0.81 mm diameter) type 2 Litz wire having 105 strands of no. 40 AWG (0.08 mm). As shown in Fig. 2(a), the coil has a circular shape and consists of two layers [5, 14].

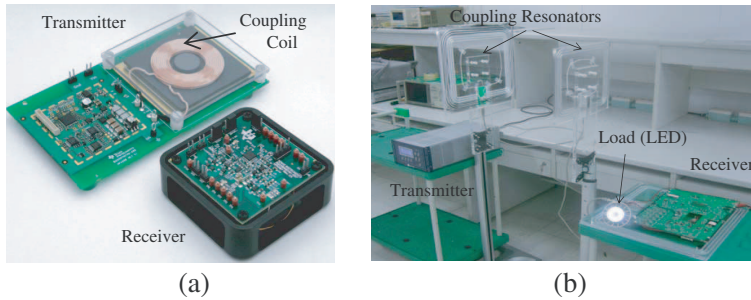


**Figure 2.** Photographs of typical LF- and HF-band wireless power transfer systems. (a) LF-band wireless power system with a transmitter and a receiver from Texas Instruments<sup>TM</sup>. (b) Demonstration using HF-band WPT system with loop resonators.

**Table 2.** Dimensions of transmitter and receiver loop resonators.

Item	Parameter	Value
Transmitter and Receiver Resonators	Number of turns	3
	Outer diameter	38 cm
	Inner diameter	33 cm
	Turn spacing	0.5 cm
Excitation loop	Number of turns	1
	Outer diameter	15 cm

On the other hand, Fig. 2(b) shows the demonstration using self-designed HF-band rectangular loop resonators [10]. The dimensions of both resonators are shown in Table 2. The sizes of resonators are selected for a size of 15-inch flat panel monitor for transmitter and receiver. By using only the outer conductor of a RG-58 coaxial cable, the rectangular three turn loop resonator is made with low parasitic impedance. Except for commercial single frequency high power sources, all circuits are designed and manufactured in our laboratory located at Kookmin University, Seoul, Korea. The operating frequency of a 13.56 MHz industrial, scientific, and medical (ISM) band was used to avoid regulation problems. Using a fixed 50 Ω nominal resistance at the both sides of the transmitter and receiver, the HF-band WPT system was successfully demonstrated. However, unexpectedly, the transmitted power became lower within a short range as the separation distance was smaller. This phenomenon is the primary motivation for this research to begin.

### 3. ISSUES ON HF-BAND WPT

#### 3.1. Simplified Analysis of HF-band WPT System

The resonant HF-band WPT system can be represented in terms of a simplified equivalent lumped circuit model as shown in Fig. 3, where the left side of the circuit is the transmitter and the right side is the receiver.

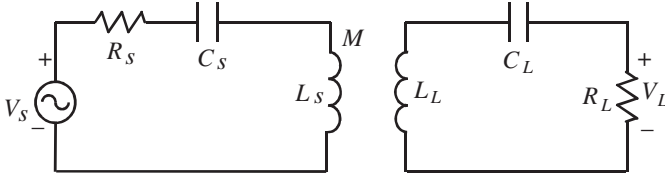


**Figure 3.** Equivalent circuit model of the series-resonant wireless power transfer system.

The equivalent circuit consists of two resonant circuits, linked magnetically by mutual impedance ( $M$ ). Starting from the left loop, the transmit loop is excited by a source with a source impedance ( $R_S$ ). A transmit resonator can be modeled as an inductor ( $L_S$ ). A capacitor ( $C_S$ ) is added to make the loop resonant at the desired frequency. Inductor  $L_S$  and  $L_L$  are connected with mutual inductance  $M$ . The receiver coil is defined similarly. Among circuit parameters in Fig. 3, only  $M$  varies as a function of the separation distance between the transmitter and receiver. Thus,  $M$  is the most important factor for designing a WPT system as it relates directly to the coupling coefficient and overall efficiency. Owing to coupled resonator theory [15], the coupling coefficient,  $k$ , can be expressed by the following:

$$k = \frac{M}{\sqrt{L_S L_L}} = \frac{f_{\text{even}}^2 - f_{\text{odd}}^2}{f_{\text{even}}^2 + f_{\text{odd}}^2}. \quad (1)$$

where,  $f_{\text{even}}$  indicates the even mode resonant frequency, and  $f_{\text{odd}}$  indicates the odd mode resonant frequency of two resonators.

Figure 3 provides a convenient reference for analysis of the transfer function of a magnetically coupled resonator system, which can be viewed as a two-port network. Using Kirchhoff's voltage law (KVL) for voltage across the load resistor  $R_L$ , one can calculate the system transfer function, which results in

$$\frac{V_L}{V_S} = \frac{j\omega M R_L}{(R_S - j/\omega C_S + j\omega L_S)(R_L - j/\omega C_L + j\omega L_L) + \omega^2 M^2}. \quad (2)$$



**Table 3.** Circuit parameters to evaluate equivalent circuit model.

Parameter	Value
$R_S, R_L$	$50 \Omega$
$L_S, L_L$	$20 \mu\text{H}$
$C_S, C_L$	Tuned to center frequency
Frequency	13.56 MHz ISM frequency

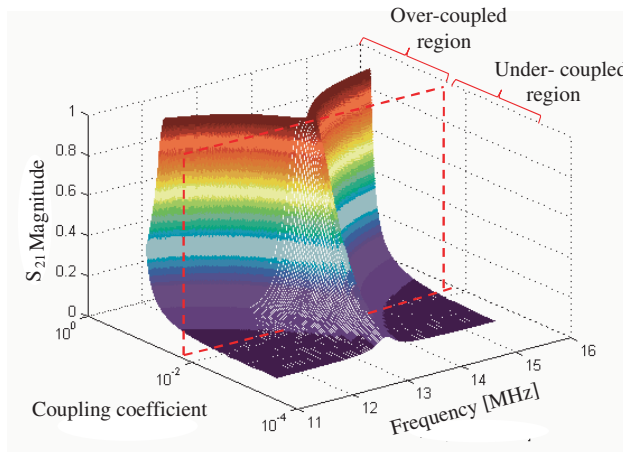


**Figure 4.**  $S_{21}$  magnitude of an HF-band WPT system’s equivalent circuit model as a function of frequency and coupling coefficient  $k$ . The circuit parameter is given in Table 2.

The system transfer function is represented in terms of linear magnitude scattering parameters ( $|S_{21}|$ ), which is important experimentally since it can be measured with a vector network analyser (VNA) [16]. Using (2), the equivalent  $S_{21}$  parameter can be calculate as

$$S_{21} = 2 \frac{V_L}{V_S} \left( \frac{R_S}{R_L} \right)^{1/2} . \tag{3}$$

The system transfer function is plotted in Fig. 4 for the circuit values shown in Table 3. This plot shows  $S_{21}$  magnitude as a function of frequency and coupling coefficient  $k$ . In Fig. 4, frequency splitting is clearly visible as the value of  $k$  is increased. As the coupling between resonators decreases, the frequency separation also decreases until the two modes converge to one. This point is called critical coupling point and represents the farthest distance at which maximum power transfer efficiency is still achievable. When  $k$  is greater than the critical point,

the system is said to be over-coupled. Conversely, when  $k$  is less than the critical point, the system is said to be under-coupled, and the delivered power to the load begins to decrease with the separation distance. If the distance between transmitter and receiver is less than the critical coupling point, the constant high efficiency versus distance can be achieved. This is the key concept of HF-band WPT systems.

### 3.2. HF-band WPT System Impedance Mismatching

Along the variation of coupling coefficients between two resonators in a short range, the load impedance of the receiver influences the transmitter. Since the overall efficiency also depends on the return loss, the input impedance variation is very important. In order to analyze these influences, the modified equivalent circuit model in Fig. 5 has been applied. Fig. 5(a) is the modified circuit model of Fig. 3 to separate from the receiver to the transmitter. And, Fig. 5(b) is the simplified equivalent circuit of Fig. 5(a) with the reflected impedance,  $Z_r$ , from the receiver for simplifying the calculation of the input impedance of transmitter [17, 18].

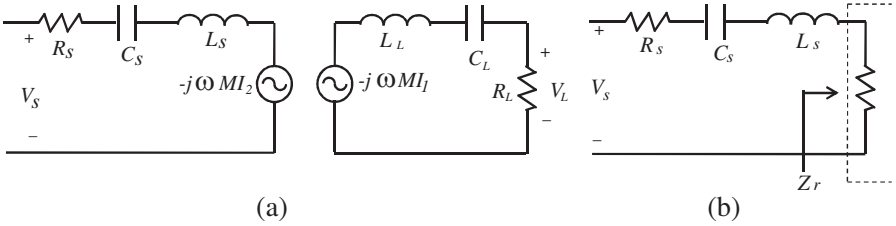


**Figure 5.** (a) Modified equivalent circuit model of Fig. 3 to separate from the receiver to the transmitter. (b) Simplified equivalent model of transmitter with the reflected impedance.

The reflected impedance is dependent on the coupling coefficient and operating frequency, and can be found by dividing the reflected voltage by the transmitter current resulting in

$$Z_r = \frac{-j\omega M I_2}{I_1} = \frac{\omega^2 M^2}{Z_2}, \quad (4)$$

where  $Z_2$  is the total impedance of receiver and is expressed by

$$Z_2 = j\omega L_L + 1/(j\omega C_L) + R_L. \quad (5)$$

Substituting (5) into (4),  $Z_r$  can be derived by

$$Z_r = \frac{\omega^4 C_L^2 M^2 R_L^2 - j\omega^3 C_L M^2 (\omega^2 C_L L_L - 1)}{(\omega^2 C_L L_L - 1)^2 + \omega^2 C_L^2 R_L^2}. \quad (6)$$

Finally, at the resonant frequency, (6) can be simplified by

$$Z_r = \frac{\omega_{res}^2 M^2}{R_L^2}. \tag{7}$$

With the reflected impedance in (7), the input impedance at resonant frequency can be calculated. As the mutual impedance is increased when two resonators are approached, the reflected impedance is increased. The power reflection efficiency ( $\eta_{11}$ ) and transmission efficiency ( $\eta_{21}$ ) are defined by (8) and (9), respectively. Therefore, overall efficiency is defined by the product of  $\eta_{11}$  and  $\eta_{21}$ . Using these equations, it can be concluded that the impedance mismatch has major effects on the overall efficiency of WPT.

$$\eta_{11} = S_{11}^2 \times 100[\%], \tag{8}$$

$$\eta_{21} = S_{21}^2 \times 100[\%]. \tag{9}$$

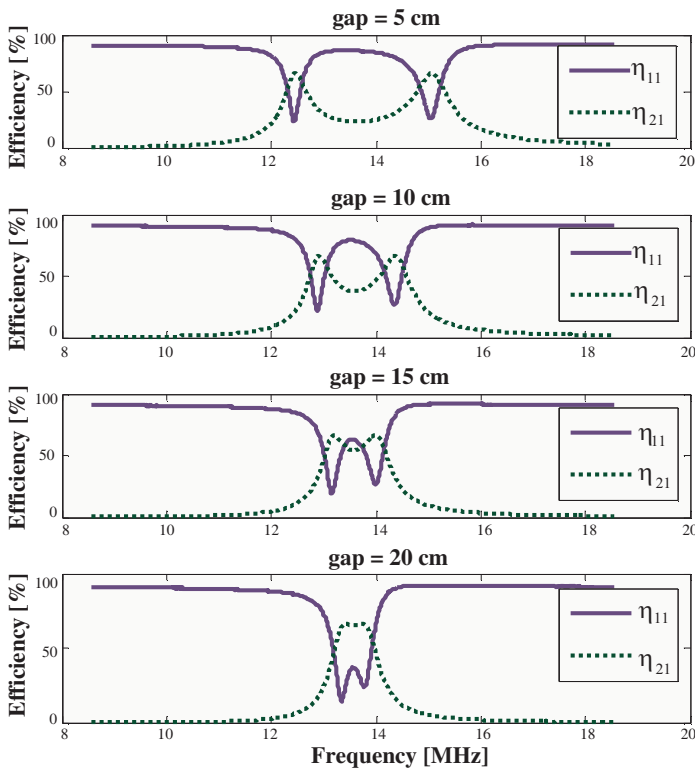


**Figure 6.** Measured results of the power reflection efficiency and transmission efficiency of the designed HF-band wireless power transfer system as a function of distance between transmitter and receiver.

In order to verify the above analysis, we designed a HF-band WPT system. A pair of single loop resonators of  $30\text{ cm} \times 30\text{ cm}$  was designed and implemented. The loop size and configuration are different from those in Table 2. This loop resonator has a low inductance value, which is equivalent to one quarter of the inductance value in Table 2. Therefore, the efficiency and range are lower than those in Fig. 4. As this system mainly focused on system design aspects of WPT, however, we have used this single loop resonator. Detailed design procedure is explained in our previous paper [10, 11].

Figure 6 shows the measured results of  $\eta_{11}$  and  $\eta_{21}$ . The frequency splitting phenomena and constant efficiency characteristics in the over-coupled region can be seen clearly. Fig. 7 also shows the loci of input return loss in the Smith chart. Because the reflected impedance only has real values at the resonant frequencies regardless of the separation distance, the loci of  $S_{11}$  of the 13.56 MHz are located in the real axis of the Smith chart. At even- and odd-modes frequencies, the loci are located near the center of the Smith chart. Therefore, good impedance matching is obtained at even- and odd-mode frequencies.

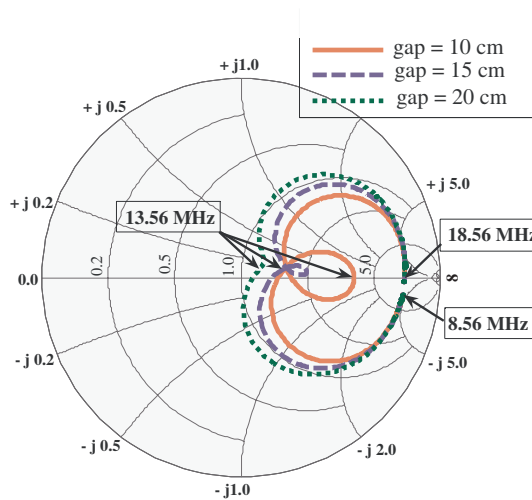


**Figure 7.** Measured  $S_{11}$  loci of designed HF-band wireless power transfer systems as the function of distance between transmitter and receiver.

### 3.3. Transmitter and Receiver Circuit Aspects

Using the over-coupled region having high coupling coefficient values, it is possible to design a HF-band WPT system with high efficiency. However, there are still technical obstacles to overcome. Generally,

as the operation frequency increases from a LF-band to a HF-band, the efficiency of the transmitter and receiver circuit decreases. For example, due to the high frequency nature of the transmitter, switching amplifier topology, such as class E, is normally implemented. Although the ideal efficiency of a class E amplifier is 100%, its real efficiency decreases due to parasitic and non-ideal components in the HF-band. Also, a class E amplifier is very sensitive to a change in load impedance. As shown in previous analysis, the load impedance ( $R_L$ ) can be transformed to varying reflected impedance ( $Z_r$ ) as a function of separation distance. This will change the output load impedance of the class-E amplifier and eventually reduce transmitter efficiency. In a LF-band WPT system, in order to reduce this effect, closed-loop drivers are normally used, which adjust their input frequency and/or duty cycle in order to compensate changes in the output load [19, 20]. However, because the operation ranges of HF-band WPT systems are very wide and their operating frequency is higher than LF-band counterparts, it is very difficult to implement closed-loop control without any communication assistance between transmitter and receiver. Maybe, the communication and control methods in a HF-band WPT system will be the next big research theme in this area.

#### **4. DESIGN ASPECTS ON HF-BAND WIRELESS POWER**

As shown in Section 3, a HF-band WPT system shows an impedance mismatch when two resonators approach each other. By reducing this effect, the efficiency of a WPT system can be enhanced. In this section, two compensation methods to overcome this effect in a short range, where large impedance mismatch occurs, are suggested. One method is to use an automatic frequency control circuit by varying the output frequency of a voltage-controlled oscillator adaptively according to the separation distance. The other method is to use a tunable impedance matching circuit using varactor diodes, which adjust impedance matching parameters according to the separation distance between two resonators.

##### **4.1. Adaptive Frequency Control Circuit**

Form previous analysis, transmission efficiency of WPT can be improved by adaptively varying the operating frequency of WPT systems as a function of separation distance. Fig. 8 shows a HF-band WPT system with an adaptive frequency control function. The

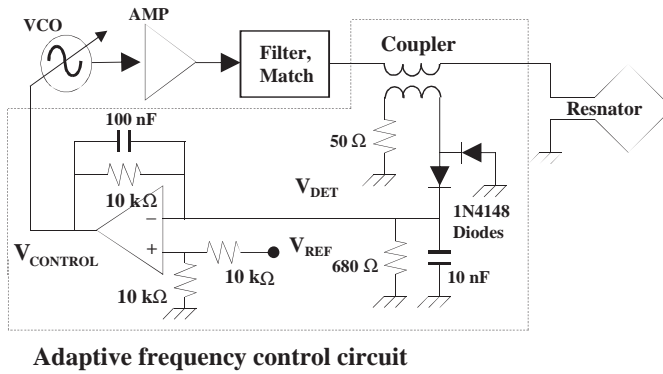


**Figure 8.** Proposed WPT system with adaptive frequency control circuit.

designed system consists of a VCO, 10 W linear power amplifier (PA), rectangular loop antennas, and feedback circuits made by a broadband directional coupler, a detector using two diodes, and a loop filter using operational amplifiers. As the separation distance between two resonating antennas decreases, the detector's output voltage ( $V_{DET}$ ) increases because of impedance mismatch. A loop filter compares it with a reference value ( $V_{REF}$ ), and the difference between two values is applied to the input of the VCO ( $V_{CONTROL}$ ) to adjust its output frequency. Among even and odd mode frequencies, VCO may be tracked to both frequencies. But, to simplify circuit design, we designed the output frequency of the VCO to be adjusted by using varactor diodes from 13.56 MHz to 15 MHz. This is an even mode frequency of WPT.

First, a typical Colpitts oscillator using 2N2222 NPN transistor and 5 V bias was designed with the output of 15 dBm. Among even and odd mode frequencies, VCO may be tracked to both two frequencies. But, to simplify circuit design, we designed the output frequency of the VCO to be adjusted by using varactor diodes from 13.56 MHz to 15 MHz.  $V_{CONTROL}$  can linearly change the output frequency of VCO [11].

Second, a broadband directional coupler operating in a HF-band is typically designed with a toroidal core or ferrite core with two holes. The directional coupler of the turn ratio of 1 : 3 using a ferrite core with two holes was designed [21]. Measured results show good broadband characteristics from 10 MHz to several hundred MHz. In the operating band, the coupling of 12.5 dB and isolation of  $-38$  dB were obtained. If the input and output port are changed, the coupled and isolated port will also be changed. So, in order to measure the effect of impedance

mismatch, a detector should be connected to the isolated port and the coupled port be terminated by  $50\ \Omega$ .

Third, we designed a linear broadband PA. Generally, HF-band PA uses power MOSFET with a class-E topology for low cost and high efficiency design. But, because a class-E amplifier generally shows narrowband characteristics, we designed the broadband amplifier using class-AB topology. Designed PA showed a 50 dB linear gain and 70% drain efficiency at 10 W output power and 13.56 MHz frequency.

Finally, a detector converts RF power of an isolated port into the direction coupler of DC voltage. General voltage doubler topology was adopted using two general purpose diodes. If the VCO is fixed at 13.56 MHz and the separation distance decreases, the detector's output voltage becomes higher because of impedance mismatch. On the other hand, if the frequency of VCO is varied to even mode frequency, the detector's output voltage is constant. Using the above circuits, a HF-band WPT system with adaptive frequency control circuits was designed and implemented, which a pair of loop antennas with a dimension of  $30\text{ cm} \times 30\text{ cm}$ . For comparison, three different frequency control methods were tested. First, the frequency was fixed at 13.56 MHz and there was no feedback function. In this case, as the separation distance became smaller, the efficiency dramatically decreased because of an impedance mismatch. Next, the VCO's control port ( $V_{\text{CONTROL}}$ ) is connected to the power supply and the voltage was adjusted manually to maximize the efficiency of the system. Finally, the adaptive frequency control circuit was activated without any manual tuning. As shown in Fig. 9, the adaptive frequency control circuit can be successfully operated. As the separation distance decreases, the operating frequency of the WPT system increases. The frequency differences between the adaptive frequency control and manual frequency control are just 200 kHz, which is only an error of 1%.

## 4.2. Tunable Impedance Matching Circuit

The drawback of the previous method is a frequency regulation issue. Generally, the frequency for WPT is bound by the ISM band. According to ISM band regulation, the usable frequency ranges are extremely small. For example, at 13.56 MHz, the range is just  $13.56\text{ MHz} \pm 7\text{ kHz}$  [22, 23]. Therefore, it is necessary to compensate the effect of the impedance mismatch without any frequency variation.

As the separation distance between two resonators decreases, the reflected impedance increases as shown in Fig. 7. But fortunately, the reflected impedance only has real values at the resonant frequencies regardless of separation distance. Therefore, it is possible to tune the impedance matching circuit using only two varactor diodes. In this

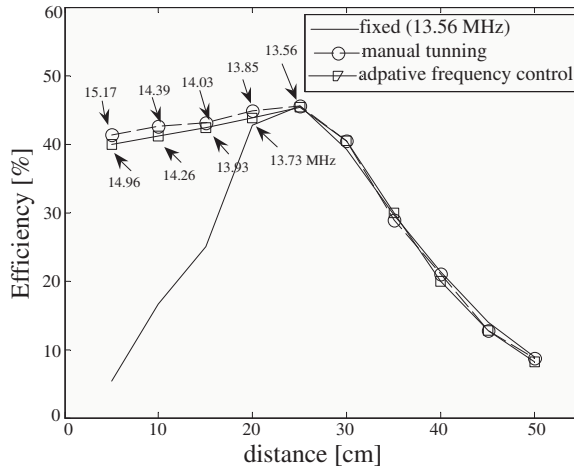


**Figure 9.** Efficiency measurement results of HF-band wireless power transfer system with three different frequency control methods.

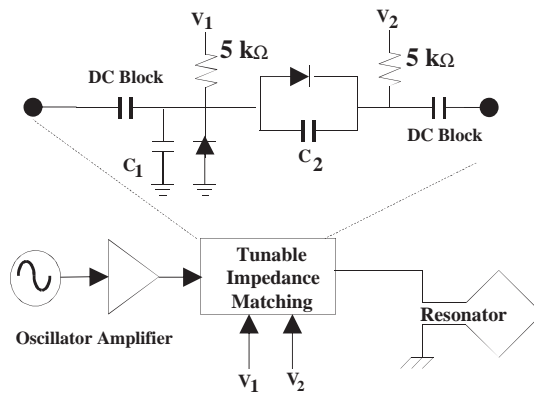


**Figure 10.** Proposed WPT system with tunable impedance matching circuit.

paper, the tunable impedance matching circuit using varactor diodes is proposed as shown in Fig. 10. A tunable impedance matching circuit is made by parallel combinations of fixed capacitors and varactor diodes (Zetex ZC836BCT-ND). In order to control the capacitance values of varactor diodes, two supply voltages are applied to  $V_1$  and  $V_2$  ports. Selected varactor diodes can vary from 195 pF at zero bias to 17 pF at 20 V bias. If a larger capacitance value is needed, the parallel combination of varactor diodes can be used. Because this method requires two control voltages, an automatic tuning technique such



**Table 4.** Capacitance and input voltage variation as a function of distance for tunable impedance matching circuit.

Item		Distance (cm)				
		40	30	20	10	5
Impedance [ $\Omega$ ]		49.86	48.4	42.05	22.6	10.9
$C_1$ [pF]		218	216.7	210.8	191.5	177.8
$C_2$ [pF]		512.8	520.4	558.3	761.6	1097
Theory	$V_1$ [V]	1.3	1.4	1.7	2.5	3.4
	$V_2 - V_1$ [V]	6.8	6.6	5.3	1.7	0.2
Measured	$V_1$ [V]	1.4	1.5	1.8	2.7	3.6
	$V_2 - V_1$ [V]	6.7	6.4	5.4	1.9	0.5

as adaptive frequency control circuits mentioned before is not easily implemented. Hence we manually adjusted two control voltages using power supply.

A HF-band WPT system with a proposed tunable impedance matching circuit was designed and implemented, which has a pair of loop resonators with a same dimension of 30 cm  $\times$  30 cm. Unlike the previous system, the parallel resonant loop resonators are used. For comparison, three different control methods are tested. First, the frequency is fixed at 13.56 MHz and there is no feedback function (Type 1). In this case, as the separation distance decreases, the efficiency decreases because of an impedance mismatch. Next, a tunable matching circuit was inserted only into the transmitter circuit and the voltage was adjusted manually to maximize the efficiency of the WPT (Type 2). Finally, tunable matching circuits were included in both transmitter and receiver sides (Type 3).

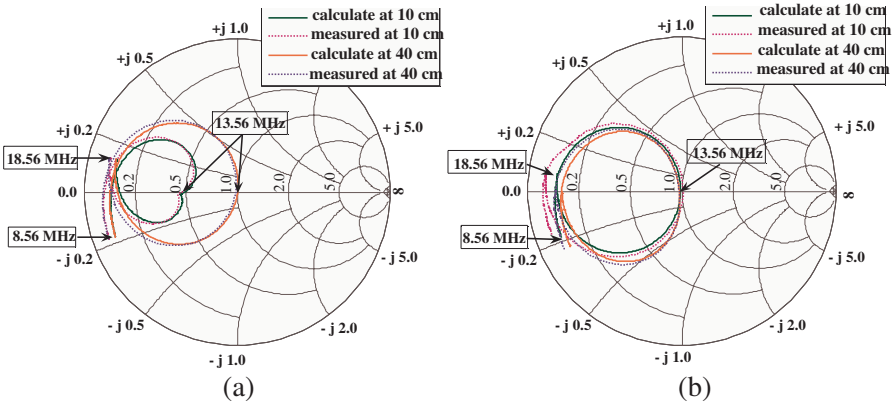
Table 4 shows the reflected impedance variations and related matching circuit parameters to compensate as a function of a distance between transmitter and receiver. Because a parallel resonant circuit was used, the separation distance was smaller and the impedance lower. Figs. 11(a) and 11(b) show the  $S_{11}$  loci in the Smith chart of Type 1 and Type 3, respectively. The loci of  $S_{22}$  of Type 1 and  $S_{22}$  of Type 2 are almost same as Fig. 11(a). Likewise, the loci of  $S_{11}$  of Type 2 and  $S_{22}$  of Type 3 are almost same as Fig. 11(b). Owing to tunable impedance matching circuits, the  $S_{11}$  and  $S_{22}$  loci of Type 3 and the  $S_{11}$  loci of Type 2 at the resonant frequency (13.56 MHz) are always located in the center of the Smith chart regardless of the separation distance.

Figure 12 shows efficiency measurement results of HF-band WPT system with three different impedance matching circuits (Type 1, Type 2, and Type 3). As expected, Type 3 shows the best efficiency

of all distances. Likewise, Type 2 shows better efficiency than Type 1.

However, because the proposed tunable impedance matching circuit requires two control voltages ( $V_1$  and  $V_2$ ), it is difficult to implement the adaptive control function like previous adaptive frequency control circuits. Therefore, some digital circuit implementation is needed. The implementation of adaptive function will be a future research topic.

Comparison of the proposed two design methods are summarized



**Figure 11.** (a)  $S_{11}$  loci at 10 cm and 40 cm distance of Type 1 system. (b)  $S_{11}$  loci at 10 cm and 40 cm distance of Type 3 system.

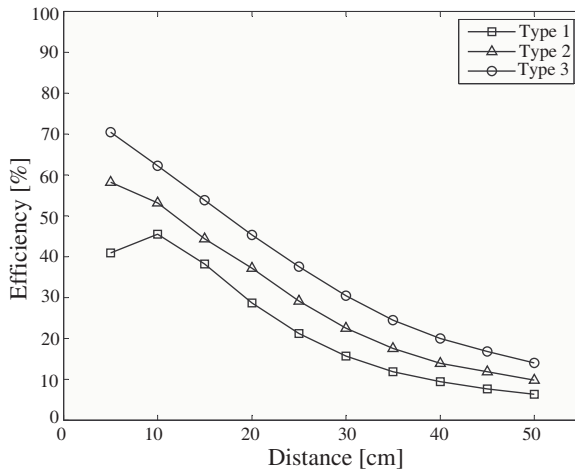


**Figure 12.** Efficiency measurement results of HF-band wireless power transfer system with three different impedance matching circuits.

**Table 5.** Comparison of design.

	Adaptive Frequency Control	Tunable Matching
Frequency regulation	- Severe limitation	- No regulation Issues
Active circuit	-Wideband design - Low efficiency	- Narrowband design - High efficiency - High power varactors
Resonator design	- Wideband design	- Narrowband design
Control	- Relatively easy - Analog implementation	- Nonlinear control - Digital implementation

in Table 5. As each system has pros and cons, HF-band WPT systems should be designed considering all these items.

## 5. CONCLUSION

This paper reviews a HF-band WPT system in comparison with a LF-band counterpart. By carefully investigating operating principles of these systems with simplified equivalent modes, it was found that maintenance of impedance matching in an over-coupled region is very important. In order to handle this mismatch, two compensation methods were suggested and high-frequency band WPT systems, with a pair of rectangular loop resonators, were designed and implemented. The input return loss and transmission efficiency were measured. From measured results, proposed methods show enhanced efficiency performance than a WPT system without any compensation techniques. Therefore, this study verifies that the proposed methods should be effective methods to enhance efficiency even though the separation distance of resonators is varied in a short range.

## ACKNOWLEDGMENT

This research was supported by the KCC (Korea Communications Commission), Korea, under the R&D program supervised by the KCA (Korea Communications Agency) (KCA-2011-11911-01110) and supported by the Korea Science and Engineering Foundation (KOSEF) grant funded by the Korea government (MEST) (No. 2011-0003543).

## REFERENCES

1. Peng, L, O. Breinbjerg, and N. A. Mortensen, "Wireless energy transfer through non-resonant magnetic coupling," *Journal of*

- Electromagnetic Waves and Applications*, Vol. 24, No. 11–12, 1587–1598, 2010.
2. Wei, X. C. and E. P. Li, “Simulation and experimental comparison of different coupling mechanisms for the wireless electricity transfer,” *Journal of Electromagnetic Waves and Applications*, Vol. 23, No. 7, 925–934, 2009.
  3. Yu, C, C.-J. Liu, B. Zhang, X. Chen, and K.-M. Huang, “An intermodulation recycling rectifier for microwave power transmission at 2.45 GHz,” *Progress In Electromagnetics Research*, Vol. 119, 435–447, 2011.
  4. Ravaud, R., G. Lemarquand, V. Lemarguand, S. I. Babic, and C. Akyel, “Mutual inductance and force exerted between thick coils,” *Progress In Electromagnetics Research*, Vol. 102, 367–380, 2010.
  5. Wireless Power Consortium, *System Description Wireless Power Transfer, Vol. I: Low Power, Part 1: Interface Definition*, Apr. 2011.
  6. Kurs, A., A. Karalis, R. Moffatt, J. D. Joannopoulos, P. Fisher, and M. Soljacic, “Wireless power transfer via strongly coupled magnetic resonances,” *Science*, Vol. 317, 83–86, Jul. 2007.
  7. [http://blogs.intel.com/research/2008/10/rattner\\_the\\_promise\\_of\\_wireless.php](http://blogs.intel.com/research/2008/10/rattner_the_promise_of_wireless.php).
  8. Choi, J. and C. Seo, “High-efficiency wireless energy transmission using magnetic resonance based on negative refractive index metamaterial,” *Progress In Electromagnetics Research*, Vol. 106, 33–47, 2010.
  9. Peng, L., J. Wang, L.-X. Ran, O. Breinbjerg, and N. A. Mortensen, “Performance analysis and experimental verification of mid-range wireless energy transfer through non-resonant magnetic coupling,” *Journal of Electromagnetic Waves and Applications*, Vol. 25, No. 5–6, 845–855, 2011.
  10. Kim, H.-S., D.-H. Won, and B.-J. Jang, “Simple design method of wireless power transfer system using 13.56 MHz loop antennas,” *Proc. ISIE Conference*, 1058–1063, Jul. 2010.
  11. Jang, B.-J. and J.-B. Lim, “Efficiency enhancement by adaptive frequency control in HF-band wireless power transfer system,” *Proc. KJMW*, 38–41, Nov. 2011.
  12. Won, D.-H., H.-S. Kim, and B.-J. Jang, “13.56 MHz wireless power transfer system using loop antennas with tunable impedance matching circuit,” *Journal of KEES*, Vol. 20, No. 5, 519–527, May 2010.

13. Kuhn, W. B. and N. M. Ibrahim, "Analysis of current crowding effects in multiturn spiral inductors," *IEEE Trans. Microwave Theory Tech.*, Vol. 49, No. 1, 31–38, Jan. 2001.
14. Texas Instruments, *bqTESLA™ Wireless Power Evaluation Kit*, Dec. 2010.
15. Wu, S.-M., C.-T. Kuo, P.-Y. Lyu, Y.-L. Shen, and C.-I. Chien, "Miniaturization design of full differential bandpass filter with coupled resonators using embedded passive device technology," *Progress in Electromagnetics Research*, Vol. 121, 365–379, 2011.
16. Barroso, J. J. and A. L. de Paula, "Retrieval of permittivity and permeability of homogeneous materials from scattering parameters," *Journal of Electromagnetic Waves and Applications*, Vol. 24, No. 11–12, 1563–1574, 2010.
17. Liu, X., W. M. Ng, C. K. Lee, and S. Y. Hui, "Optimal operation of contactless transformers with resonance in secondary circuits," *IEEE 23th Applied Power Electronics Conference and Exposition*, 645–650, Feb. 2008.
18. Wang, C.-S., G. A. Covic, and O. H. Stielau, "Power transfer capability and bifurcation phenomena of loosely coupled inductive power transfer system," *IEEE Trans. Ind. Electron.*, Vol. 51, No. 1, 148–157, Feb. 2004.
19. Vandevoorde, G. and R. Puers, "Wireless energy transfer for stand-alone systems: A comparison between and high power applicability," *Sensors and Actuators A: Physical*, Vol. 92, No. 1–3, 305–311, Elsevier, Aug. 2001.
20. Low, Z. N., J. J. Casanova, P. H. Maier, J. A. Taylor, R. A. Chinga, and J. Lin, "Method of load/fault detection for loosely coupled planar wireless power transfer system with power delivery tracking," *IEEE Trans. Ind. Electron.*, Vol. 57, No. 4, 1478–1486, 2010.
21. Piatnitsa, V., D. Kholodnyak, I. Fischuk, M. Komulainen, H. Jantunen, and I. Vendik, "Miniature 90° and 180° directional couplers for Bluetooth and WLAN applications designed as multilayer microwave integrated circuits," *Journal of Electromagnetic Waves and Applications*, Vol. 25, No. 2–3, 169–175, 2011.
22. FCC 47 CFR, *Part 18-Industrial, Scientific, and Medical Equipment*, 1998.
23. Naz, M. Y., A. Ghaffa, N. U. Rehman, S. Naseer, and M. Zakaullas, "Double and triple Langmuir probes measurements in inductively coupled nitrogen plasma," *Progress In Electromagnetics Research*, Vol. 114, 113–128, 2011.